

## MODELING OF CHEMISTRY AND ROCK ALTERATION AT A DEEP-SEATED GEOTHERMAL FIELD

M. SATO<sup>\*1</sup>, S. WHITE<sup>\*2</sup>, K. OSATO<sup>\*1</sup>, T. SATO<sup>\*1</sup>, T. OKABE<sup>\*1</sup>, N. DOI<sup>\*3</sup>, K. KOIDE<sup>\*4</sup>

<sup>\*1</sup> Geothermal Energy Research & Development Co., Ltd., 11-7, Kabuto-cho, Nihonbashi, Chuo-ku, Tokyo, Japan.

<sup>\*2</sup> Industrial Research Limited (IRL), PO Box 31 310, Lower Hutt, New Zealand.

<sup>\*3</sup> Japan Metals & Chemicals Co., Ltd. (JMC) Ukai, Takizawa-mura, Iwate, 020-01, Japan.

<sup>\*4</sup> New Energy and Industrial Technology Development Organization, Sunshine 60, 30F, 3-1-1, Higashi-Ikebukuro, Toshima-ku, Tokyo, Japan.

### ABSTRACT

The project "Deep-Seated Geothermal Resources Survey" has been performed by the New Energy and Industry Technology Development Organization (NEDO). This project investigated the development of deep geothermal resources. As part of this project we have investigated the feasibility of developing numerical models of deep-seated geothermal reservoirs. Of particular interest are the conditions beneath the explored area of existing reservoirs. The numerical models match not only temperature and pressure measurements but also a number of chemical and geological conditions of the developed reservoir. These conditions appear to be more sensitive to the deep reservoir properties than temperature and pressure.

For this work, we have used a version of TOUGH2 (Pruess, 1991) that has been modified to include the transport of reacting chemicals (White, 1995). We model a simplified conceptual model of the Kakkonda geothermal field which is located northern part of Japan. Exploratory drilling beneath the produced area of the field found temperatures that exceeded 350°C.

Firstly a model is developed with the permeabilities and geothermal inflow adjusted to provide a good match to temperature data taken from the shallow part of the reservoir. Next we add sources of volcanic gases (H<sub>2</sub>S, CO<sub>2</sub>, HCl) at the top of the two-phase area that forms over the intrusion. Finally we calculate reservoir chemistry and adjust gas source strength to match reservoir chemical conditions. A model with permeability of the order of 10<sup>-16</sup>m<sup>2</sup> to a depth of about 3km is capable of representing the observed hydrothermal alteration reservoir chemistry and temperature distribution. A reasonable match to measured isograds of alteration such as lumontite, wairakeite was obtained. The key to matching alteration is the existence of a source of magmatic vapor. Reservoir chemistry is sensitive to the distance of this source from the observed reservoir.

### INTRODUCTION

For many years it has been possible to compute the transport of heat and mass within the earth using simulators such as TOUGH2 and TETRAD. Reaction-path simulators are also well advanced, and used as a matter of course by geochemists to unravel the intricacies of the chemistry of fluids within the earth (e.g. Reed 1982, Parkhurst 1995). Recently there has been a growing interest in combining these disciplines to allow the modeling of reactive chemical transport in porous media (e.g. Lichtner 1992, Steefel and Lasaga 1995, White 1995 and Lichner and Seth 1996).

In this paper, we have applied the reactive transport simulator CHEM-TOUGH2 to the Kakkonda system. The aim of this work was to develop two numerical models of Kakkonda geothermal reservoir that match temperature and pressure measurements. In one of these models the deep (below 2 km) permeability is set to a small value and in the other it is varied to ensure a good match to measured pressures and temperatures. These may be insensitive to the properties of the deep reservoir. Once the models were developed then they were extended so that they matched not only pressure and temperature measurements but also matched a number of chemical and geological conditions of the developed reservoir. These conditions appear to be more sensitive to the deep reservoir properties than temperature and pressure.

### CONVECTION SYSTEM OF THE GEOTHERMAL FIELD

Because there is a large amount of published data on the Kakkonda field (Geothermics, 1998), we have used this as a basis for a generic, liquid dominated, geothermal field. The aim of this work is not to produce a realistic model of the Kakkonda field, but rather to investigate the role of deep permeability on

shallow (<2 km depth) chemistry and hydrothermal alteration.

The Kakkonda geothermal field is located about 600km northeast of Tokyo and is one of the most active liquid-dominated fields in Japan. The history of production from the field and the hydrology of the production zones are described in some detail in McGuinness et al. (1995).

Recent drilling at Kakkonda has found a large neogranitic pluton of 0.34 to 0.07 Ma at a depth of 2000 - 2800m. The well WD-1, drilled as part of the Japanese national project “Deep-Seated Geothermal Resources Survey”, together with other deep wells drilled nearby by JMC provide a unique insight into the structure and conditions beneath an active geothermal reservoir.

### CONCEPTUAL MODEL OF THE GEOTHERMAL FIELD

The model has a horizontal length of eight kilometers and reaches to a depth of 3.5km. At the surface we assume water containing no dissolved solids or gases, a pH of 7, a constant temperature of 15°C and a pressure of one bar. The vertical boundaries of the model are no-flow of mass or heat.

The bottom boundary does not permit the flow of mass but does allow the flow of heat, the temperature distribution is fixed at that shown in Figure 1. This temperature distribution is based on that of Doi et al. (1998). The modeled region is divided horizontally into twenty layers each with a thickness of 175m. Each layer is divided into 25 elements. These elements are smallest at the left of the model and larger towards the right boundary. We have allowed for quite a complex permeability structure as shown in Figure 1.

We developed two models. The first, hereinafter referred to as Scenario 1 allows the permeability in the deep reservoir to be adjusted. The second, Scenario 2, fixes the deep permeability at a low value. For the scenario 2 the permeability of rocks below 1.5km was set to  $10^{-18} \text{ m}^2$  and the above process repeated while fixing the permeabilities of regions labeled Rock 3, Rock4, Rock 5 and Rock 6 in Figure 1. The initial geology of the reservoir, shown in Figure 2, is a simplification of that presented in Doi et al. (1998). The reservoir is divided into the four zones (Granite, Cordierite, Biotite, and Rest. Minerals present in each zone are shown in Table 1.

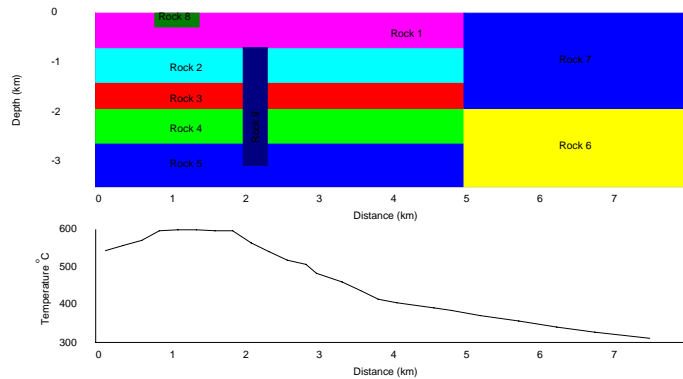


Figure 1: Permeability distribution and bottom temperature used for Kakkonda model

Table 1: Initial mineral assemblage

Zone	Quartz	Albite	Anorthite	k-Feldspar	annite	cordierite	enstatite
Granite	yes	yes	yes	yes			
Cordierite	yes	yes	yes	yes		yes	
Biotite	yes	yes	yes	yes	yes	yes	yes
Rest	yes	yes	yes	some			

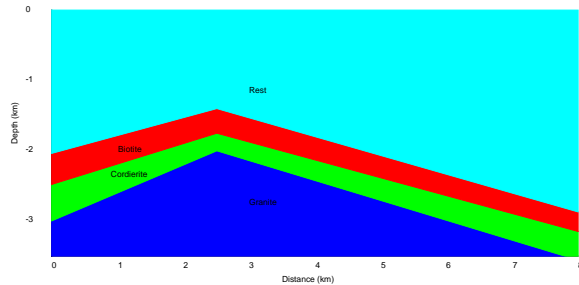


Figure 2 Initial geology

## CHEMICAL ENVIRONMENT

The hydrothermal environment within or immediately adjacent to shallow (< 4km) cooling diorite plutons is characterised by high temperatures (up to 1100°C), pressures ranging from hydrostatic to lithostatic (200 – 2000 bar), and by the presence of highly reactive fluids. In this work, we consider only the interaction between the volatile species released from a cooling magma, and the overlying hydrothermal environments. It is assumed that metamorphic rock alteration is complete before the period modeled begins.

Modeling the transport of reactive chemicals is a computer intensive activity, and requires that a balance be struck between chemical complexity and calculation time. For this work, we modeled the reservoir in terms of  $H_2O$ ,  $H^+$ ,  $Cl^-$ ,  $SO_4^{2-}$ ,  $HCO_3^-$ ,  $HS^-$ ,  $SiO_2(aq)$ ,  $Al^{+++}$ ,  $Ca^{++}$ ,  $Mg^{++}$ ,  $K^+$ ,  $Fe^{++}$  and  $Na^+$  component species. These fluid components allow the modeling of reactions between the main magmatic volatiles ( $CO_2$ ,  $SO_2$ ,  $H_2S$ ,  $HCl$ ) and the most common rock-forming minerals (albite, anorthite, K-feldspar and quartz) and also most of the minerals in the metamorphic alteration zones. Twenty-five of the most prevalent secondary aqueous species and a total of 14 minerals are also considered (Table 2).

Table2: All minerals considered in the calculation

Mineral	Formula
albite	$NaAlSi_3O_8$
alunite	$KAl_3(SO_4)_2(OH)_6$
anhydrite	$CaSO_4$
annite	$KFe_3(Si_3AlO_{10})(OH)_2$
anorthite	$CaAl_2Si_2O_8$
k-feldspar	$KAlSi_3O_8$
quartz	$SiO_2$
cordierite	$Mg_2Al_3(AlSi_5)O_{18}$
calcite	$CaCO_3$
enstatite	$MgSiO_3$
muscovite	$KAl_2(AlSi_3O_{10})(OH)_2$
laumontite	$Ca(Al_2Si_4O_{12}) \cdot 4H_2O$
pyrite	$FeS_2$
wairakit	$Ca(Al_2Si_4)O_{12} \cdot 2H_2O$

Simplifying assumptions adopted in the treatment are:

- chemical equilibrium is maintained;
- gas phase chemistry is ignored;
- reservoir permeability is isotropic (fracture flow is ignored).

We believe the assumption of chemical equilibrium to be justified in the hot area of the reservoir, but this assumption is certainly invalid in the cool areas. For example, the pH in the cool surface waters is much higher than normally found in shallow areas of geothermal reservoirs, but is correct for water in equilibrium with the assumed rock assemblage at 15°C.

The SOLTHERM database (Reed 1992) provides equilibrium constants as a function of temperature for all the reactions considered in this work up to a temperature of 350°C. It appears none of the widely available chemical databases provides data above this temperature explicitly. The program SUPCRT92 (Johnson et al. 1992) and associated databases provide a theoretical prediction of equilibrium constants for almost all the reactions of interest at higher temperatures (up to 415° C). There is excellent agreement between theoretical predictions of SUPCRT92 and the SOLTHERM database in regions where they overlap. For charged species it is not possible to calculate the activity coefficients for charged species near the critical point of water. The approach we have taken is to calculate equilibrium constants and activity coefficients along a contour in T,P space that defines these numbers for all temperatures up to 425°C. Above this temperature all there is no flow of fluids as rock permeability is reduced to very low values by the transition to plastic behavior by the rock.

## MODELING SOFTWARE

For this work we have used a version of TOUGH2 (Pruess 1991) that has been modified to include the transport of reacting chemicals (White 1995). The original code was capable modeling temperatures up to 350°C and pressures up to 100 MPa. This has been extended to temperatures up to 800°C but the pressure limit of 100 MPa remains (White and Mroczek 1998).

We have ignored the solubility of all neutral aqueous species in the gas phase even though it may be significant between 360 - 374°C with pressures on the saturation line. Carbon dioxide and hydrogen sulfide gases are included in the simulation as is the effect they have on the saturation pressure of water.

## **MODELING RESULTS**

### **Initial match to measured temperatures**

There are three base models, one for scenario 1 and two for scenario 2. These will be referred to as model 1, model 2 and model 3. The parameters for the regions of these models defined in Figure 1 are summarised in Table 3. And we take four conditions of mass fluxes of magmatic vapor (Run1-4) summarised in Table 4. Model 1 has been developed allowing moderate permeabilities in the deep reservoir. Note, however, that we have included a temperature dependent permeability so the permeability of areas of the reservoir where the temperature is greater than 400° C is very small. A source of magmatic vapor is included in the model.

Model 2 fixes the permeability below 1500m to a low value but does allow the input of magmatic gases into the model, the temperature on the bottom boundary is fixed at that estimated in Doi et al. (1998). Model 3 does not allow passage of magmatic gases into the shallow reservoir at all. The bottom boundary temperature for model 3 is increased significantly over those in models 1 and 2.

Table 3: Rock properties for the three models. In all cases in specific heat was set to 10<sup>3</sup> J/kg/°C and the porosity to 0.1.

Material	Porosity	Model 1 permeability	Model 2 permeability	Model 3 permeability
Rock 1	0.1	1.0×10 <sup>-14</sup>	1.0×10 <sup>-14</sup>	1.0×10 <sup>-14</sup>
Rock 2	0.1	1.0×10 <sup>-14</sup>	1.0×10 <sup>-14</sup>	1.0×10 <sup>-14</sup>
Rock 3	0.1	1.0×10 <sup>-15</sup>	1.0×10 <sup>-18</sup>	1.0×10 <sup>-18</sup>
Rock 4	0.1	2.0×10 <sup>-16</sup>	2.0×10 <sup>-18</sup>	2.0×10 <sup>-18</sup>
Rock 5	0.1	1.0×10 <sup>-16</sup>	1.0×10 <sup>-18</sup>	1.0×10 <sup>-18</sup>
Rock 6	0.1	1.0×10 <sup>-16</sup>	1.0×10 <sup>-18</sup>	1.0×10 <sup>-16</sup>
Rock 7	0.1	1.0×10 <sup>-17</sup>	1.0×10 <sup>-17</sup>	1.0×10 <sup>-17</sup>
Rock 8	0.1	5.0×10 <sup>-16</sup>	5.0×10 <sup>-16</sup>	5.0×10 <sup>-16</sup>
Rock 9	0.1	1.0×10 <sup>-17</sup>	1.0×10 <sup>-17</sup>	1.0×10 <sup>-17</sup>

Table 4: Mass flux of magmatic vapor for the model runs

Run	Model	Mass flux of magmatic vapor (kg/m <sup>2</sup> /s)
1	1	6.5×10 <sup>-6</sup>
2	2	1.0×10 <sup>-5</sup>
3	2	0.0
4	3	0.0

In Figures 2-4 we present the initial state temperatures, also shown on these figures are measured temperatures taken from Doi et al. (1998). With model 1 a two-phase zone was formed immediately above the intrusion. The temperatures in this zone were from about 360°C to the critical point. This two-phase zone would be high in CO<sub>2</sub> and H<sub>2</sub>S and there is some support for the existence of such a zone from the H<sub>2</sub>S and CO<sub>2</sub> found during the drilling

of WD-1. No two-phase zone was formed with model 2 or model 3.

These figures show that it is possible to get similar temperatures in the shallow reservoir with a number of different assumptions about the conditions at depth.

### **Chemical matching**

For each of these models the chemical conditions in the reservoir were calculated using the states in Figures 3-5 equilibrated with the mineral distribution as an initial state. For the models that included sources of volcanic gas then chemical components representing volcanic gas were included in the model, tables 5 and 6 give the chemical component fluxes for models 1 and 2. In model 1 these sources were included at the top of the two-phase zone. For model 2 these sources were added at a depth of 1500m. This is at the bottom of the permeable section of the reservoir.

Table 5: Chemical component fluxes from magmatic vapor for model 1

Species	Flux kg/m <sup>2</sup> /s	Enthalpy (J/kg)
H <sub>2</sub> O	6.45×10 <sup>-7</sup>	2.5×10 <sup>6</sup>
H <sup>+</sup>	2.06×10 <sup>-9</sup>	2.5×10 <sup>6</sup>
Cl <sup>-</sup>	4.1×10 <sup>-9</sup>	2.5×10 <sup>6</sup>
SO <sub>4</sub>	1.6×10 <sup>-8</sup>	2.5×10 <sup>6</sup>
HCO <sub>3</sub> <sup>-</sup>	4.6×10 <sup>-10</sup>	2.5×10 <sup>6</sup>
HS <sup>-</sup>	9.9×10 <sup>-9</sup>	2.5×10 <sup>6</sup>

Table 6: Chemical component fluxes from magmatic vapor for model 2

Species	Flux kg/m <sup>2</sup> /s	Enthalpy (J/kg)
H <sub>2</sub> O	1.00×10 <sup>-6</sup>	2.7×10 <sup>6</sup>
H <sup>+</sup>	6.20×10 <sup>-10</sup>	2.7×10 <sup>6</sup>
Cl <sup>-</sup>	1.2×10 <sup>-9</sup>	2.7×10 <sup>6</sup>
SO <sub>4</sub>	4.7×10 <sup>-9</sup>	2.7×10 <sup>6</sup>
HCO <sub>3</sub> <sup>-</sup>	1.4×10 <sup>-10</sup>	2.7×10 <sup>6</sup>
HS <sup>-</sup>	3.0×10 <sup>-9</sup>	2.7×10 <sup>6</sup>

Results of the modeling are summarized in Figures 6-9. Runs 3 and 4 are not viable candidates to represent the reservoir. The effect of low permeability on Run 2 can be seen clearly in figure 7 and figure 9. The Cl<sup>-</sup> concentration is lower at the shallower parts of the reservoir. In Run 1 the convective system reaches to the top of the pluton and transports the magmatic volatile into shallower parts of the reservoir. The pH is much higher for Run 1 than Run 2. The pH is in the range 6-7 in the upflow zones and 9-12 in the upper reservoir and downflow zones. This matches reasonably well to the values published by Yanagiya et al. (1996). Once the results of Yanagiya et al. (1996) have been corrected to reservoir conditions pH in the range 6-7 are typical for the deep reservoir. The high Cl<sup>-</sup> concentration is shown at the top of the pluton. It represents the contribution of the Cl<sup>-</sup> from the magmatic vapor. The pH and Cl<sup>-</sup>

contours depict the shape of the convective upwelling over the intrusion.

Figures 10-12 show the calculated distribution of some key minerals overlaid on a cross-section of the field showing observed hydrothermal alteration for Run 1 and Run 2. In neither case is the match to the anhydrite distribution very good although the results for Run 1 do have the correct shape the minimum depth at which anhydrite exists is below the observed value. There are two possible explanations for this, either the upflow area at the left of the model is too weak and dilution by the downflow causes undersaturation with respect to anhydrite or the equilibrium assumption is causing too rapid a precipitation of anhydrite.

In Run 2 anhydrite is deposited in the area magmatic vapor enters the system but it does not seem to be transported in the upflow regions. The match to Wairakite is better for Run 1 than Run 2 although the isograd is below the observed level. Both Run 1 and Run 2 match the laumontite isograd reasonably well.

## **DISCUSSION**

We have investigated the feasibility of developing numerical models of deep-seated geothermal fields from a geochemical point of view, taking the case of the Kakkonda geothermal field. Although the results do not necessarily agree exactly with measured data, the approach gives supplementary information on the deep-seated geothermal reservoir. The conclusions that can be drawn from the present work are summarized as follows.

- (1) A model with permeability of the order of  $10^{-16} \text{ m}^2$  to a depth of about 3km is capable of representing the observed hydrothermal alteration, reservoir chemistry and temperature distribution better than a model with a permeability of  $10^{-18}$  below 1.5km.
- (2) In order to match observed rock alteration with a model that had low permeability at depth we needed to include a source of magmatic vapor. If the permeability of the deep rocks is less than  $10^{-19} \text{ m}^2$  then this source is unlikely to be present.
- (3) The key to matching the hydrothermal alteration in the shallow reservoir is a source of magmatic vapor.

## **REFERENCES**

Christenson, B.W., Wood, C.P., Arehart, G.B. (1998), "Shallow magmatic degassing: Processes and PTX constraints for paleo-fluids associated with the Ngatamariki diorite intrusion", New Zealand. Proc. 9<sup>th</sup> Int. Sym. On Water-Rock Interaction. (Arehart and Hulston (eds) Balkema (Pub.))

Doi, N., Kato, O., Ikeuchi, K., Komatsu, R., Miyazaki, S., Akaku, K., Uchida, T. (1998), "Genesis of the plutonic-hydrothermal system around quaternary granite in the Kakkonda geothermal system, Japan", *Geothermics*, **27**(5), 663-690.

Geothermics. (1998), Special issue Deep geothermal systems Japanese national project in Kakkonda.

Hanano, M. (1995), "Hydrothermal convection system of the Kakkonda geothermal field, Japan", *Proc World Geoth. Congress Florence, Italy, 1629-1634*.

Hanano, M., Seth, M.S. (1995), "Numerical modeling of hydrothermal convection systems including supercritical fluid", *Proc World Geoth. Congress Florence, Italy, 1681-1686*.

Johnson J.W., Oelkers, E.H., Helgeson, H.C. (1992), "SUPCRT92: A software Package for Calculating the Standard Molal Thermodynamic Properties of Minerals, Gases, Aqueous Species and Reactions from 1 to 5000 Bar and 0 to 1000° C", *Computers & Geosciences*, **18**, 7.

Lichtner, P.C. and Seth, M.S. (1996), "Multiphase-multicomponent nonisothermal reactive transport in partially saturated porous media", Presented at the International Conference on Geological Disposal of Radioactive Waste, Canadian Nuclear Society. Sept 16-19 Winnipeg Manitoba, Canada.

Lichtner, P.C. (1992), "Time-space continuum description of fluid/rock interaction in permeable media", *Water Resour. Res.*, **28**, 3135-3155.

McGuinness, M.J., White, S.P., Young, R.M., Ishizaki, H., Ikeuchi, K., Yoshida, Y. (1995), "A Model of the Kakkonda Geothermal Reservoir", *Geothermics*, **24**, 1-48.

Moore, G., Vennemann, T., Carmichael, I.S.E. (1995), "Solubility of water in magmas to 2 kbar", *Geology*, **95**, 12, 1099-1102.

Parkhurst, D.L. (1995), "User's guide to PHREEQC, a computer model for speciation, reaction path, advective-transport and inverse geochemical calculations", U.S. Geological Survey Water-Resources Investigation Report, 95-4227, 143.

Pruess, K. (1991), "TOUGH2 - A general-purpose numerical simulator for multiphase fluid and heat flow", *Rep LBL-29400*, Lawrence Berkeley Lab., Berkeley, Calif.

Reed, M.H. (1982), "Calculation of multicomponent chemical equilibria and reaction processes in systems involving minerals, gases and an aqueous phase", *Geochim. et Cosmo. Acta*, **46**, 513-528.

Steeffel, C.I. and Lasaga, A.C. (1994), "A coupled model for transport of multiple chemical species and kinetic precipitation/dissolution reactions with applications to reactive flow in single phase hydrothermal system", *Am. J. Sci.*, **294**, 529-592.

White, S. P. (1995), "Multiphase non-isothermal transport of systems of reacting chemicals", *Water Resour. Res.*, **31**, 1761-1772

Yanagiya, S., Kasai, K, Brown, K.L., Giggenbach, W.F. (1996), "Chemical Characteristics of Deep geothermal Fluid in the Kakkonda Geothermal System, Iwate Prefecture, Japan", *Chinetsu*, **33**, 1.

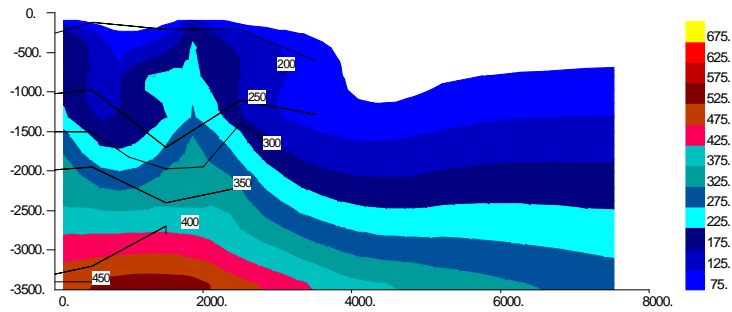


Figure 3: Calculated temperatures ( $^{\circ}\text{C}$ ) for Model 1. The contours indicate measured temperatures and the colors model results.

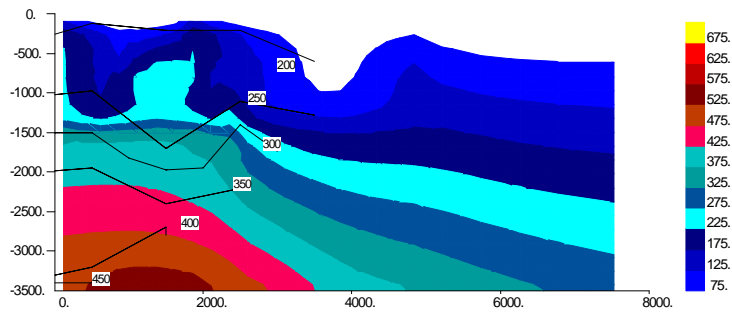


Figure 4: Calculated temperatures ( $^{\circ}\text{C}$ ) for Model 2. The contours indicate measured Temperatures and the colors model results.

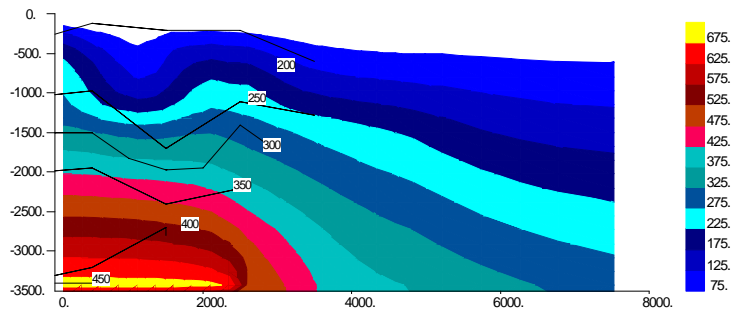


Figure 5: Calculated temperatures ( $^{\circ}\text{C}$ ) for Model 3. The contours indicate measured Temperatures and the colors model results.

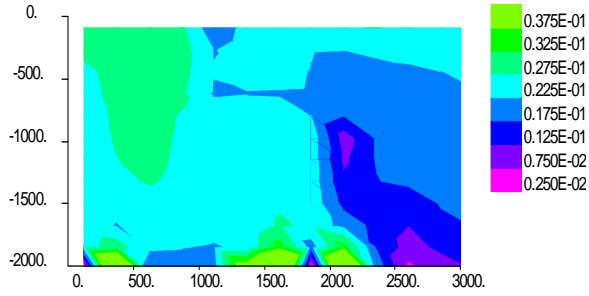


Figure 6: Cl<sup>-</sup> concentrations for run 1 after 10,000 years , units are moles/dm<sup>3</sup>

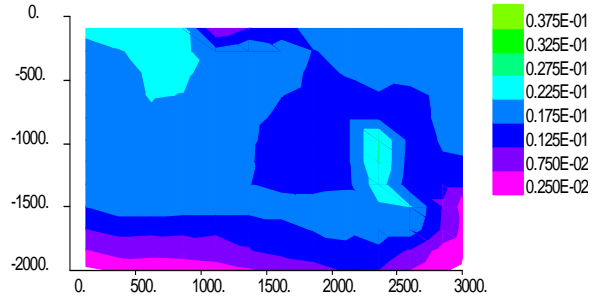


Figure 7: Cl<sup>-</sup> concentrations for Run2 after 10,000 years , units are moles/dm<sup>3</sup> of fluid

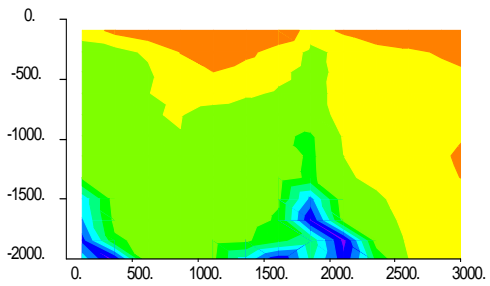


Figure 8:pH for run1 after 10,000 years,

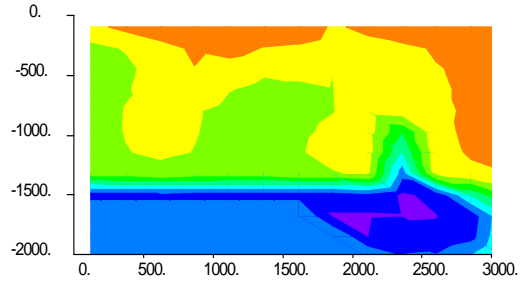


Figure 9: pH for Run2 after 10,000 years,

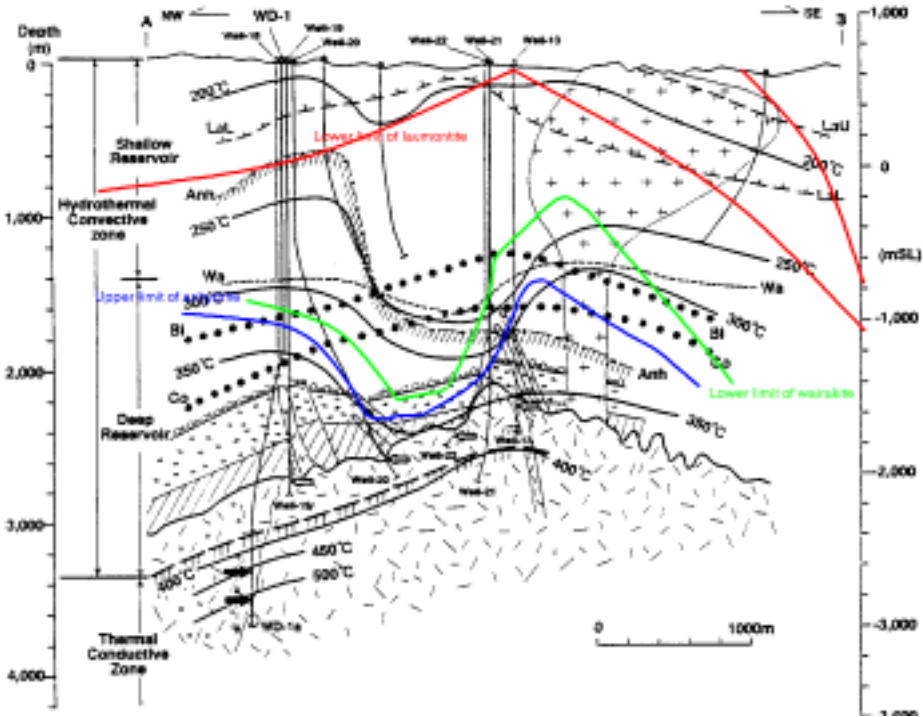


Figure 10: Calculated location of some minerals in Run 1. Calculated values are shown in colour. The base diagram is taken from Doi *et. al* (1998).

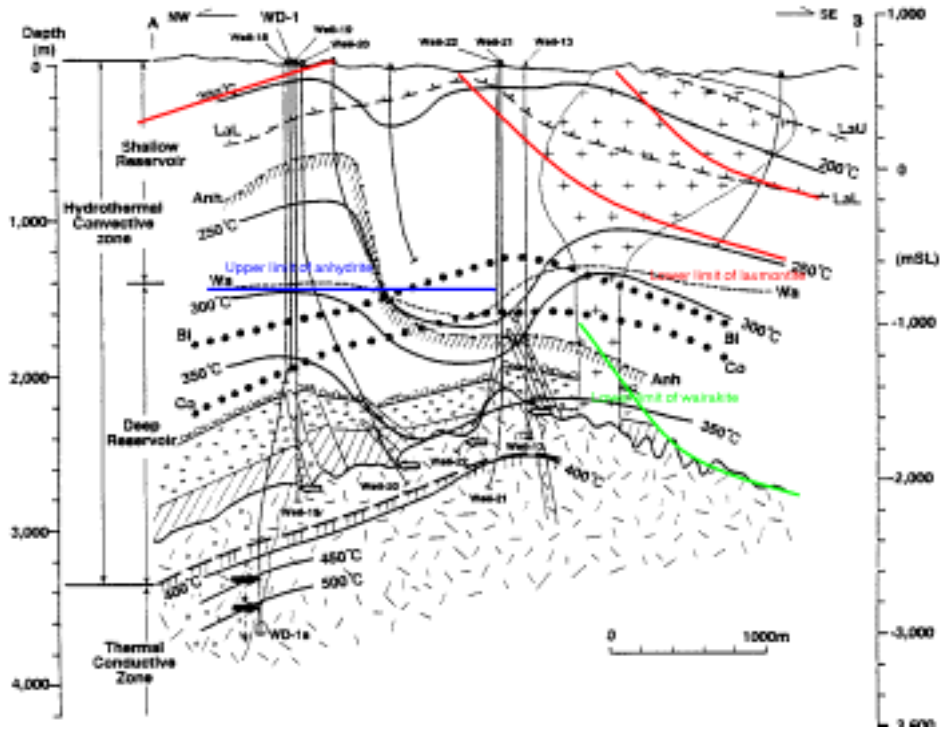


Figure 11: Calculated location of some minerals in Run 2

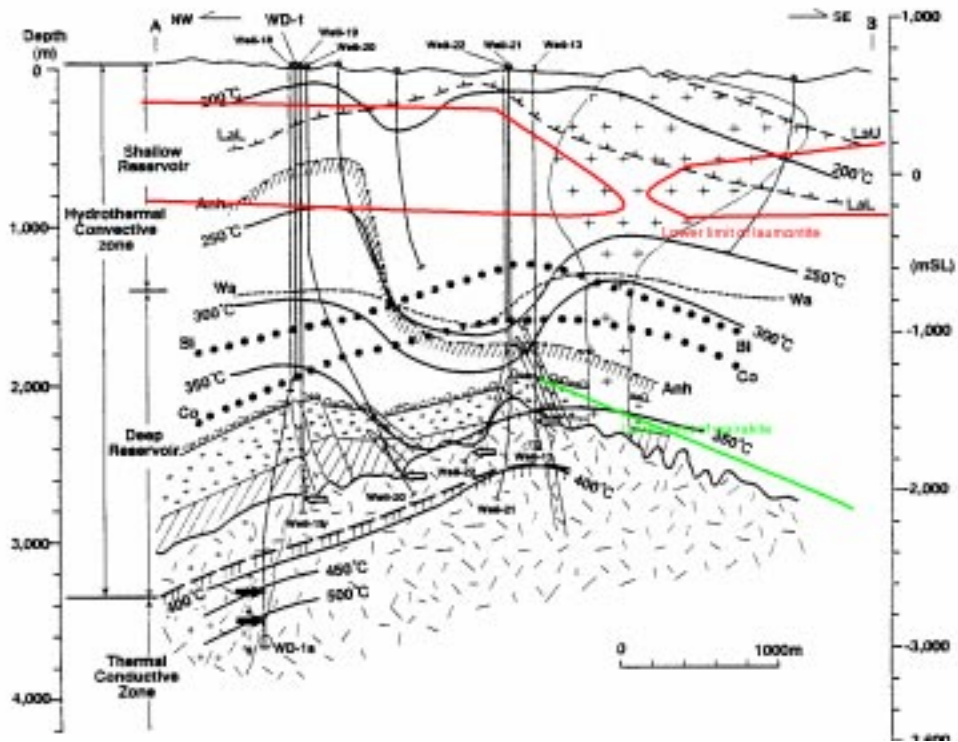


Figure 12: Calculated location of some minerals in Run 3